FOKKER-PLANCK MODELLING OF ECCD FOR NTM STABILISATION IN ITER

F. Volpe, B. Lloyd and M.R. O'Brien

EURATOM/UKAEA Fusion Association, Culham Science Centre
Abingdon, Oxon, OX14 3DB, United Kingdom

e-mail: volpe@ukaea.org.uk

Abstract

The relativistic and self-consistent ray tracing and Fokker-Planck code BANDIT-3D is used to study the capability of the ITER ECRH upper launchers to stabilise m/n=2/1, 3/2 neo-classical tearing modes. We compare the efficiency of the upper and lower row of mirrors and study the effect of density and temperature variations. The geometry of the launcher (including astigmatism and remote steering) is taken into account. It is also proved that the 8 beams in the launcher can be effectively combined to yield a localised driven current that increases linearly with power over the range investigated (up to 10MW per beam).

1 Introduction

Neo-classical tearing modes (NTMs) are observed to limit the achievable long-pulse β to values well below the ideal magneto-hydrodynamic limit in low collisionality plasmas. However, their suppression by means of localised ECCD has also been observed in several tokamaks (see review in Ref.[1]). For these reasons, NTM control through localised ECCD is envisaged as one of the key applications of the ITER ECRH 170GHz system [2].

In the present study the linear and surface density of driven current were adopted as "figures of merit" to quantify the efficiency of NTM stabilisation. The launch angles yielding maximum figures of merit at the q=3/2 and q=2 surfaces for a standard reference ITER scenario were identified by means of ray tracing and Fokker-Planck calculations, whose numerical and geometrical aspects are treated in Secs.2-3. Such an optimisation was done for the upper and lower row of mirrors, which are compared in Sec.4, and was repeated for various peak densities and temperatures (Sec.5). Finally, since `BANDIT-3D` is a non-linear Fokker-Planck code, it was possible to check that non-linear effects at high gyrotron power, even up to 10MW per beam, are negligible for the present ITER and antenna designs (Sec.6).

2 Numerical Method

`BANDIT-3D` is a relativistic and self-consistent ray tracing and Fokker-Planck code [3, 4]. Trapping effects play an important role for NTMs be-

cause the rational surfaces of interest are relatively close to the plasma boundary. In BANDIT-3D, trapping effects are modelled in a realistic up-down asymmetric single null divertor configuration. The equilibrium for ITER "scenario 2" (Q=10, 15MA, inductive, B_0=5.3T, T_{e0}=24.8keV, n_{e0}=1.02 $\times 10^{20} m^{-3}$) [5] was imported from EFIT. The density, temperature and Z_{eff} profiles were tabulated by ASTRA against the square root of the normalised *toroidal* flux, ρ. Subsequently they were splined and replaced with profiles of enhanced resolution in the range ρ=0.5-1 containing the rational surfaces of interest, q=2 and q=3/2.

3 Beam Geometry

The broadening of a gaussian beam of waist radius w_0 and wavelength λ as the longitudinal co-ordinate z along the beam increases, is described by [6]: $w = w_0\sqrt{1+(z\lambda/\pi w_0^2)}$. For the ITER ECRH upper launcher $\lambda \simeq$ 1.8mm and $w_0 >$ 70mm. Therefore, with good approximation the beam radius grows *linearly* with z in the deposition region, located at $z \gtrsim$1.5m from the launcher. This allows the gaussian beam to be treated as a bundle of independent rays[1]. The total beam power, 1MW, was distributed among the rays according to a gaussian distribution, with the intensity at the edge of the cone equal to e^{-2} times its value at the centre.

Each bundle consists indeed of 8 groups of 20 coplanar, equally spaced rays. The 8 planes intersect in the beam axis and are also equally spaced in angular separation. It was empirically found that 8 planes capture the anisotropy associated with the fact that the plasma refracts different parts of the beam differently, therefore even cylindrically symmetric beams generally acquire non-circular sections.

In addition to this *refraction*-induced astigmatism, automatically included in the *ray*-tracing, the anisotropic focusing strength of the last mirror introduces some natural astigmatism. The latter was modelled by applying different geometrical optics approximations to each of the 8 planes. The foci and angular apertures were determined by linear fits in the absorption region, in order to find the best approximations where the current is driven. Focal spreads as large as 171 and 284mm were found respectively for the lower and upper row of mirrors. They bring significant corrections when compared to the beam length of about 1.5m from the last mirror to the deposition region.

Remote steering was also taken into account. The ITER Upper Launcher

[1]Rays are independent in the ray tracing part, meaning that diffraction is neglected, thus ray trajectories are independent. Rays, however, are not independent in the FP part of the code, in the sense that the total driven current is not just the sum of the driven currents: the FP solver takes into account the total deposited power and the $k_{\|}$ spectrum resulting from all the rays.

features steerable mirrors at the transmission line *input* [7]. As the beam exits the transmission line with a variable angle, it hits the last, fixed mirror, in different positions. The virtual point sources for the ray bundles move accordingly. Their displacement was calculated and included in the initial conditions for the ray tracing.

4 Numerical results for upper and lower row of mirrors

Ray tracing and FP calculations were performed for different launch angles from the lower and upper row of mirrors of the ITER ECRH Upper Launcher.

The toroidal launch angle β defined in Ref.[8] was varied in the interval 10-30^o in steps of 2^o . For each value of β, a *regula falsi* algorithm [9] was used to identify the optimal poloidal launch angle α for driving maximum current I at ρ=0.656 and ρ=0.778. Such values were indicated by ASTRA as the locations of the rational surfaces q=3/2 and q=2.

The full width d of the current profile was computed as the distance between the two locations where the current density profile $j(\rho)$ equals $1/e$ times its peak value. From fig.2a and 3a one can deduce which launch angles yield the highest figure of merit, I/d, for NTM stabilisation via *modulated* CD [8, 10]. The corresponding points have been circled in fig.1. Ellipses encompassing more than one point refer to broad maxima (e.g. the maximum at β=18-24^o for NTM 3/2, lower row). Similarly, I/d^2 plots in fig.2b and 3b show the best angles in the case of *non-modulated* CD [8, 10]. The corresponding points have been framed in fig.1.

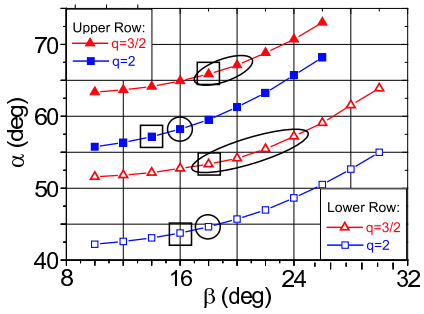

Fig.1: Poloidal launch angles for NTM 2/1 and 3/2 stabilisation, as functions of the toroidal angle. The highest I/d and I/d^2 are achieved in the points highlighted by 🖵 and □ respectively.

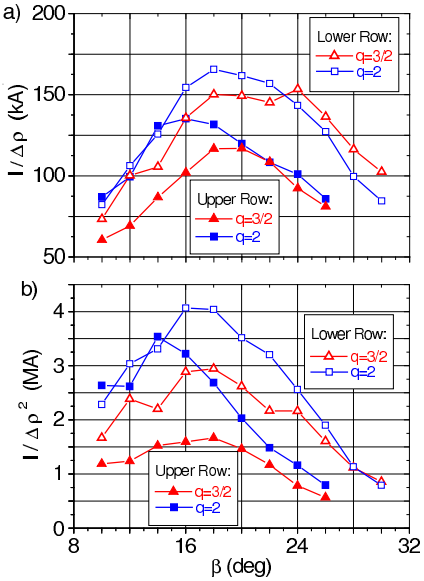

Fig.2: Figures of merit for NTM stabilisation by means of modulated (a) and non-modulated (b) ECCD

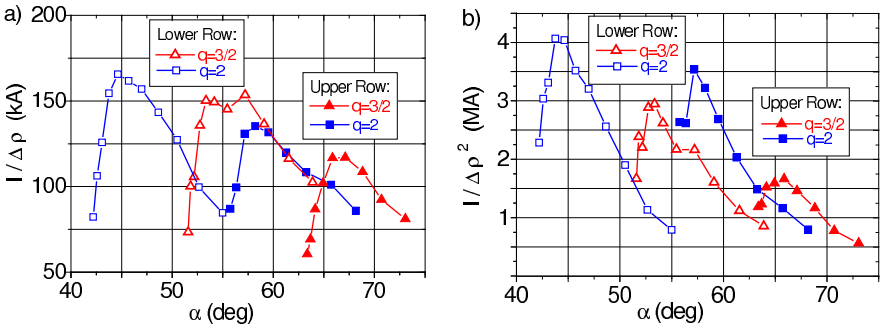

Fig. 3: Like fig.2 but as function of the poloidal launch angle

The highest I/d^2 are reached at lower values of β than the highest I/d, because d plays a bigger role and its increase (the broadening of the beam) is less pronounced for a more perpendicular launch, i.e. at smaller β.

From fig.1, one infers the need for poloidal steering ranges of 8^o and 9^o at fixed β, for the upper and lower row respectively, for ITER scenario 2. Changes of magnetic configuration and of plasma parameters such as density and temperature will further broaden the required steering range. On the other hand, here each row is supposed to control both the $q = 2$ and $q = 3/2$ surfaces (not simultaneously, of course). A narrower range will be sufficient for a mirror dedicated to a single rational surface.

Finally, it is interesting to compare the performances of the lower and upper row and note that the latter reaches lower values of I/d and I/d^2, mainly because of the wider d. In turn, this is a consequence of the relative position of the mirrors and of the target, resulting in longer -and, therefore, broader- beams from the upper row. A slightly reduced current also contributes to the difference.

The upper and lower row achieve their highest NTM stabilisation efficiency at different β. A comparison of record values, regardless of the value of β at which they are achieved, gives an upper/lower row deterioration of 19% for I/d and of 13% for I/d^2 for q=2. For q=3/2 the I/d deterioration amounts to 24% and that of I/d^2 to 43%. It is noted that the use of a slightly higher frequency for the upper row could move the resonance to a more favourable position, shorten the beam path length and thus reduce the disparity between the upper and lower rows.

5 Effect of change of density and temperature

To investigate the effect of the local density and temperature, the study presented in the previous section was repeated for different n_e and T_e profiles while keeping fixed the plasma equilibrium and the beam model (mirror location and focusing strength). The new profiles were obtained by rescal-

ing the given ones by a numerical factor between 0.7 and 1.3. In this way, their shape was preserved. This is not realistic at the plasma centre, as the profile peaking is expected to change. However we deal with deposition at $\rho = 0.656$ and 0.778, thus the waves do not encounter the core plasma where n_e and T_e may be unrealistic.

The first aspect to be studied was the influence of the density and temperature variation on the optimal poloidal launch angle α. The effect of $\Delta n_e/n_e$ was found to be negligible, with corrections of less than 0.25^o for the values of β of interest, β=14-24^o .

The effect of $\Delta T_e/T_e$ on α is stronger, up to 1^o , but is still smaller or much smaller than the experimental steering range and is comparable with the precision of simulations, as $\sim 1^o$ is also the disagreement among different codes [8].

Another part of the study focused on the figures of merit I/d and I/d^2 as functions of β for different $\Delta n_e/n_e$ and $\Delta T_e/T_e$. The decrease of I/d and I/d^2 as n_e increases and their increase with T_e are in accord with the fact that the ECCD efficiency scales as T_e/n_e.

6 Multiple beams and non-linear corrections at high power

The separate launch from the lower (L) and upper (U) row of mirrors was compared with simultaneous launch (L+U). The current driven for the latter case was found to be just the sum of the currents driven for separate L and U launch. The only exception is an 8% degradation of I when targeting the q=3/2 surface. Moreover, as expected the beam width $\Delta\rho$ for simultaneous launch is intermediate between the values of $\Delta\rho$ for separate launch.

Not only are the currents for L and U launch additive, but also beams from the same row can be combined in a single beam of intensity equal to the sum of the intensities. This saves computational time. Thanks to toroidal symmetry, one can shift toroidally all the mirrors arrayed in a certain row and simulate a single beam of power equal to the sum of the powers. In this way, the power density is artificially increased by a factor 4 and it is important to check that this does not introduce non-linearities.

Moreover, although the power density will not dramatically change because of focusing, which is already at the limit allowed by the trade-off between improved localisation and reduced steering range [7] and will therefore undergo only minor modifications, it could increase because of a unit gyrotron power increase from 1MW to 1.5 or 2MW.

For these reasons, it was checked with the non-linear Fokker-Planck code `BANDIT-3D` that the driven current is proportional to the injected power even up to 10MW per beam, in agreement with results for earlier ITER designs [11].

Summary and Conclusions

Ray tracing and Fokker-Planck calculations were carried out to study the intensity and localisation of the current driven by the ITER ECRH Upper Launcher at the q=2 and 3/2 rational surfaces, in order to stabilise the corresponding neoclassical tearing modes (NTMs).

The beam was modelled as a bundle of rays originating in a virtual rotation point. Then astigmatic corrections were introduced to account for the anisotropic focusing strength of the last mirror.

The simulations were performed from the lower and upper row of mirrors of the Upper Launcher and it was found that the lower row is more efficient in stabilising the NTMs, primarily because of the better CD localisation. It was also found that their combined use leads to a current profile that is just the sum of the current profiles from the separate rows.

Density variations were found to have negligible influence on the launch direction, whereas temperature changes may lead to corrections of up to 1^{o} . The driven current varies approximately as T_e/n_e, as expected.

Finally, it was confirmed that non-linearities at high power are negligible, even up to 10MW per beam.

Acknowledgements

This work is jointly funded by the UK Engineering and Physical Sciences Research Council and EURATOM. The work is being carried out under the EFDA Technology Task TW3-TPH-ECHULA in collaboration with other EURATOM Associations.

References

[1] B. Lloyd, Proc.14th Topical Conf. on RF Power in Plasmas, Oxnard (2001) 33
[2] H. Zohm, this conference; H. Zohm *et al.*, this conference
[3] J. S. McKenzie, M.R. O'Brien, M. Cox, Comp.Phys.Comm. 1991, **66**, 194
[4] M.R. O'Brien *et al.*, Proc. IAEA Technical Meeting on Advances in Simulation and Modelling of Thermonuclear Plasmas, Montreal (1992) p.527
[5] Y. Gribov, private communication
[6] P.F. Goldsmith, *Quasioptical Systems*, IEEE Press Piscataway 1998
[7] A.G.A. Verhoeven *et al.*, this conference
[8] G. Ramponi *et al.*, Proc.IAEA Technical Meeting on ECRH Physics and Technology for ITER, 14-16 July 2003, Kloster Seeon (Germany)
[9] W.H. Press *et al.*, *Numerical Recipes in Fortran* (Cambridge Univ. Press 1992)
[10] G. Giruzzi *et al.*, Nucl. Fus. 1999, **39**, 107
[11] R.W. Harvey *et al.*, Nucl. Fus. 1997, **37**, 69 and references therein